AD-A191 009 METHOD FOR PREDICTION AND DETERMINATION OF TAKEOFF 1/1
PERFORMANCE FOR VECTORED THRUST VEHICLES(U) NAVAL AIR
TEST CENTER PATUXENT RIVER MD J F CALVERT 05 JAN 88
UNCLASSIFIED NATC-TM-87-171-SA F/G 1/2 NL

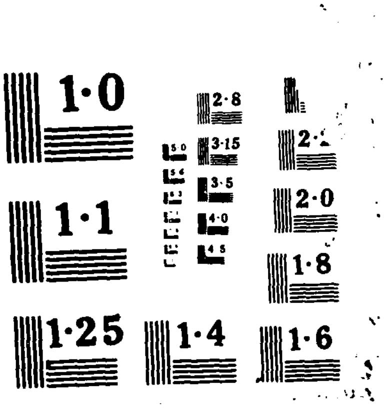
1·0
2·8
3·15
5·0
5·6
3·5
4·0
4·5
2·2
2·0
1·1
1·8
1·25
1·4
1·6

AD-A191 809

[illegible] TEST CENTER

[illegible] MARYLAND

88 2 25 070

NAVAL AIR TEST CENTER
PATUXENT RIVER, MARYLAND

The Naval Air Test Center (NAVAIRTESTCEN) is continually studying sponsor satisfaction. To facilitate this study, we would appreciate your views and opinions by completing this questionnaire. With sufficient response, this will alleviate the need for our semi-annual surveys, as well as provide us with a more meaningful evaluation of performance. *Please complete the questionnaire, fold, staple, and return it to the address on the reverse side.* All responses will remain confidential and are to be utilized by NAVAIRTESTCEN personnel only

---

SPONSOR SATISFACTION INDEX

DATE	PROGRAM	WORK UNIT	SPONSOR

LEGEND FOR RATING CRITERIA:

5	- *Substantially above average*	2	- *Marginal*
4	- *Above Average*	1	- *Unaccountable/Unsatisfactory*
3	- *Average*		

FACTOR	DEFINITION/CONSIDERATIONS	RATING
COST	REASONABLENESS OF ESTIMATES/CHARGES *(ARE RATES COMPETITIVE?)*	
FINANCIAL MANAGEMENT	DO FINAL BILLINGS APPROXIMATE THE NEGOTIATED TARGETS? ARE AMPLE TIME AND JUSTIFICATION GIVEN WHEN ADDITIONAL FUNDS ARE REQUIRED?	
SCHEDULE	ARE OPERATIONS/DELIVERABLES CONDUCTED/PROVIDED WITHIN THE NEGOTIATED TIME FRAMES?	
RESPONSIVENESS	ARE QUESTIONS ANSWERED? CHANGES ACCOMMODATED AND TECHNICAL PRODUCTS PRODUCED WITHIN EXPECTATIONS?	
TECHNICAL PERFORMANCE EFFECTIVENESS	EFFECTIVENESS AND TECHNICAL QUALITY OF PRODUCTS AND SERVICES PROVIDED?	
OVERALL SATISFACTION	DEGREE OF SATISFACTION WITH NAVAIRTESTCEN'S OVERALL PERFORMANCE ON YOUR PROGRAM.	

COMMENTS

OFFICIAL BUSINESS
PENALTY FOR PRIVATE USE, $300

POSTAGE & FEES PAID

DEPARTMENT OF THE NAVY
DOD-316

COMMANDER, NAVAL AIR TEST CENTER
(Code CT251M)
NAVAL AIR TEST CENTER
PATUXENT RIVER, MD 20670-5304

REPORT DOCUMENTATION PAGE

READ INSTRUCTIONS BEFORE COMPLETING FORM

1. REPORT NUMBER TM 87-171 SA	2. GOVT ACCESSION NO.	3. RECIPIENT'S CATALOG NUMBER
4. TITLE (and Subtitle) METHOD FOR PREDICTION AND DETERMINATION OF TAKEOFF PERFORMANCE FOR VECTORED THRUST VEHICLES		5. TYPE OF REPORT & PERIOD COVERED TECHNICAL MEMORANDUM 6. PERFORMING ORG. REPORT NUMBER
7. AUTHOR(s) MR. J. F. CALVERT		8. CONTRACT OR GRANT NUMBER(s)
9. PERFORMING ORGANIZATION NAME AND ADDRESS NAVAL AIR TEST CENTER STRIKE AIRCRAFT TEST DIRECTORATE PATUXENT RIVER, MARYLAND 20670-5304		10. PROGRAM ELEMENT, PROJECT, TASK AREA & WORK UNIT NUMBERS A511-5115/053-2/5257-000-696 A5511B314
11. CONTROLLING OFFICE NAME AND ADDRESS NAVAL AIR TEST CENTER DEPARTMENT OF THE NAVY PATUXENT RIVER, MARYLAND 20670-5304		12. REPORT DATE 5 JANUARY 1988 13. NUMBER OF PAGES 16
14. MONITORING AGENCY NAME & ADDRESS (if different from Controlling Office)		15. SECURITY CLASS. (of this report) UNCLASSIFIED 15a. DECLASSIFICATION DOWNGRADING SCHEDULE

16. DISTRIBUTION STATEMENT (of this Report)

APPROVED FOR PUBLIC RELEASE; DISTRIBUTION UNLIMITED.

17. DISTRIBUTION STATEMENT (of the abstract entered in Block 20, if different from Report)

18. SUPPLEMENTARY NOTES

19. KEY WORDS (Continue on reverse side if necessary and identify by block number)

VSTOL TAKEOFF PERFORMANCE

20. ABSTRACT (Continue on reverse side if necessary and identify by block number)

YAV-8B and AV-8B Short Takeoff (STO) test results had indicated that STO techniques for the Harrier II could be further optimized, particularly for operations at higher hover weight ratios (1.3 and above). This paper documents a method to predict and determine optimum land-based STO performance with minimum flight testing required. The method was applied during the determination of the optimum STO performance of the AV-8B, and is tailored generally toward thrust vectored vehicles with rapid thrust vectoring capability. With certain assumptions accounted for this approach can also be used in less restricted cases. Emphasis was placed on developing a

DD FORM 1 JAN 73 1473 EDITION OF 1 NOV 65 IS OBSOLETE

Cont

20.

repeatable task terminating with sufficient flight path acceleration at 50 ft AGL. STO tests conducted using the revised STO procedures validated the improvement in STO performance. Changes to the AV-8B flight operations manual were recommended in order to implement the revised STO task.

SUMMARY

YAV-8B and AV-8B Short Takeoff (STO) test results had indicated that STO techniques for the Harrier II could be further optimized, particularly for operations at higher hover weight ratios (1.3 and above). This paper documents a method to predict and determine optimum land-based STO performance with minimum flight testing required. The method was applied during the determination of the optimum STO performance of the AV-8B, and is tailored generally toward thrust vectored vehicles with rapid thrust vectoring capability. With certain assumptions accounted for this approach can also be used in less restricted cases. Emphasis was placed on developing a repeatable task terminating with sufficient flight path acceleration at 50 ft AGL. STO tests conducted using the revised STO procedures validated the improvement in STO performance. Changes to the AV-8B flight operations manual were recommended in order to implement the revised STO task.

DTIC
COPY
INSPECTED
6

Accesion For
NTIS CRA&I ☒
DTIC TAB ☐
Unannounced ☐
Justification ....
By ....
Distribution /
Availability Codes
Dist | Avail and / or Special
A-1

METHOD FOR THE DETERMINATION AND OPTIMIZATION OF VECTORED THRUST TAKEOFF PERFORMANCE

J. F. Calvert
Strike Aircraft Test Directorate
Naval Air Test Center
Patuxent River, Maryland 20670

Abstract

YAV-8B and AV-8B Short Takeoff (STO) test results had indicated that STO techniques for the Harrier II could be further optimized, particularly for operations at higher hover weight ratios (1.3 and above). This paper documents a method to predict and determine optimum land based STO performance with minimum flight testing required. The method was applied during the determination of the optimum STO performance of the AV-8B, and is tailored generally toward thrust vectored vehicles with rapid thrust vectoring capability. With certain assumptions accounted for this approach can also be used in less restricted cases. Emphasis was placed on developing a repeatable task terminating with sufficient flight path acceleration at 50 ft above ground level. Short takeoff tests conducted using the revised STO procedures validated the improvement in STO performance. Changes to the AV-8B flight operations manual were recommended in order to implement the revised STO task.

Nomenclature

Symbol	Description
a	net acceleration
$(a/g)_D$	normalized flight path acceleration for aircraft at weight W_D
$(a/g)_L$	normalized flight path acceleration for aircraft at weight W_L
C_D	aircraft drag coefficient
C_L	aircraft lift coefficient
C_{D_g}	aircraft drag coefficient in ground effect
C_{L_g}	aircraft lift coefficient in ground effect
D	aerodynamic drag
D_g	drag evaluated in ground effect
D_M	momentum drag (total mass flow rate times vehicle airspeed)
F	the net force acting in the flight path direction
F_{avg}	average net non-conservative force between V_{to}
and	occurring at $\sqrt{([V_{50}^2+V_{to}^2]/2)}$
h_1	height at initial position
h_2	height at final position
Δh	height or altitude difference between initial and final conditions
L	aerodynamic lift
L_g	average aerodynamic lift evaluated in ground effect
L_t	total lift (aerodynamic and thrust generated lift)
m	aircraft mass
M	average total mass flow rate through engine
S	wing reference area
S_d	integral path distance, ground roll distance
$S_e(\%)$	estimated percent error in ground roll distance
due to	the instantaneous takeoff assumption
S_v	ground roll distance to velocity for thrust vectoring
S_g	ground roll distance to takeoff
S_c	estimated distance from V_v to V_{to}
S_{fp}	air distance traveled along the flight path to 50 ft AGL
S_{ap}	ground distance traveled for climbout to 50 ft AGL
m	aircraft mass
M	mass flow rate of air through the engine
T	installed net thrust,
T_g	installed gross thrust,
Δt	time difference between initial and final conditions
V	airspeed
$V_{a/g}$	velocity for minimum acceptable a/g
V_{to}	*takeoff velocity*
V_y	vertical airspeed
V_v	velocity for engine thrust vectoring to target θ_j during takeoff run
V_{nr}	nozzle rotation velocity (same as V_v)
W	gross weight
W_C	aircraft weight in climbing flight
W_D	desired weight for weight correction
W_L	aircraft weight in level flight
W_1	gross weight at initial height
W_2	gross weight at final height
W/W_h	hover weight ratio (aircraft weight divided by maximum weight at which the aircraft can hover
for	given ambient conditions)
x	aircraft c.g. position
α	aircraft angle of attack
γ	flight path angle without wind correction
γ_g	flight path angle corrected for wind affects
Λ	average aircraft ground roll acceleration (evaluated at $V_{to}/\sqrt{2}$ if assumed constant)
μ	dynamic coefficient of surface friction
θ_j	angle between line of thrust and fuselage reference line (thrust vector angle)
ρ	ambient density
Φ	average acceleration from V_v to V_{to}

Introduction

This paper develops and presents an approach to predicting and determining optimum Short Takeoff performance for rapid thrust vectoring vehicles. STO performance refers to velocity and distance required to takeoff, velocity and distance required to clear an obstacle, and the velocity at which thrust is vectored during ground roll initiating takeoff. Unlike conventional takeoff testing, it is difficult to separate STO testing of vectored thrust aircraft into distinct flying qualities and performance areas. A repeatable STO task is directly dependent upon both aircraft performance and STO technique (which includes climbout as well as takeoff). The approach outlined for predicting STO performance involves optimization of the parameters relative to lift, drag, thrust, and flight path acceleration. Optimization also accounts for the requirements for quick and precise attitude capture, attitude control and maximum rate of climb. The developed flight test method for determination of optimum STO performance was applied to the AV-8B Harrier II aircraft. Method and results are presented herein.

Prediction of Short Takeoff Performance

Objective

Basic performance prediction is achieved through a mathematical analysis of the governing equations. STO performance should be optimized for full operational capability within the given performance and handling limitations of the aircraft concerned. By identifying the variables required for STO performance prediction, separation of the variables into task dependent and airframe dependent categories can be achieved. The STO task can then be developed accounting for both performance and controllability. It is important to remember that controllability greatly affects the airborne distance required to clear a given obstacle.

Short Takeoff Profile

The typical short takeoff profile (figure 1) for rapid thrust vectoring vehicles generally consists of the ground roll phase, a brief thrust rotation-takeoff-position capture phase, and the climbout-acceleration-transition phase. Vectored thrust minimizes ground roll distance to takeoff by augmenting wing lift with thrust lift. This concept has been adopted for use in certain land based, shipboard, and restricted area operations.

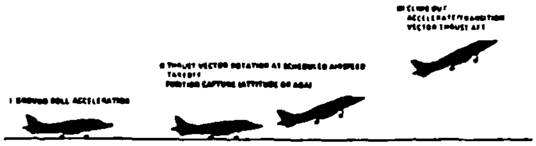
I GROUND ROLL ACCELERATION
II THRUST VECTOR ROTATION AT SCHEDULED AIRSPEED
TAKEOFF
POSITION CAPTURE (ATTITUDE OR AOA)
III CLIMB OUT
ACCELERATE/TRANSITION
VECTOR THRUST AFT

Figure 1 Typical Short Takeoff Profile

Takeoff Ground Roll Distance Prediction

Ground roll distance can be predicted by applying the work-energy relationship. For basic terms this relationship states

$$\int(\text{work}) = \int(\text{energy})$$
$$\int F \cdot ds = \Delta KE + \Delta PE$$

where F = non-conservative forces acting on the body
ΔPE = change in potential energy from initial state to final state
ΔKE = change in kinetic energy from initial state to final state

The forces acting on an aircraft during the takeoff ground roll are shown in figure 2. Applying the work-energy relationship,

$$\int[T\cos(\theta_j+\alpha) - D_g - \mu(W - L - T\sin(\theta_j+\alpha))]\cdot dS_d = WV_{to}^2/(2g) - W\Delta h \quad (1)$$

To reduce the complexity of the integral certain assumptions can be applied. First, assume T is constant over the ground run, with the constant value taken where velocity is equal to $V_{to}/\sqrt{2}$ (average between initial and final conditions). This is a valid assumption for jet aircraft during the ground run (reference 1). Second, assume W is constant over the ground run. The validity of this assumption depends upon the initial gross weight of the aircraft, the fuel flow required for takeoff thrust rating, and the time required (distance required) to takeoff. Because the velocity vector direction is not changing during the ground roll, assume α remains fairly constant over the takeoff ground roll.

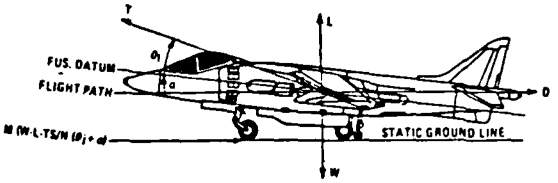

Figure 2 Forces On Aircraft During Ground Roll

Since most runways have little or no slope, Δh is negligible, therefore assume $\Delta PE = 0$. Fix the thrust vector angle during takeoff at an angle less than 20 deg relative to the velocity vector during the ground roll and assume that momentum drag and gross thrust are reasonably parallel to the velocity vector (as assumed in figure 1, however for clearness θ_j is shown out of scale). For aircraft with rapid thrust vector capability, thrust should remain aft for the takeoff ground run in order to maximize acceleration and minimize ground roll distance. At thrust vector rotation velocity, thrust would be vectored such that takeoff would occur rapidly with sufficient flight path acceleration. For slow vector thrust capability (such as tilt rotor aircraft), θ_j would most likely remain fixed throughout the takeoff. If θ_j does not remain below 20 deg, then the assumption that momentum drag and gross thrust are parallel to the velocity vector is no longer valid. In that case, the net thrust term needs to be separated into the momentum drag and gross thrust components such that the momentum drag is accounted for in the direction of the aerodynamic drag and the gross thrust is accounted for in the vectored thrust direction. This differs from conventional takeoff and landing aircraft where the thrust remains fairly parallel with the velocity vector.

Integrating equation (1) using the above assumptions, and recalling from basic aerodynamics that drag and lift are equal to $1/2\rho V^2 SC_D$ and $1/2\rho V^2 SC_L$, respectively, the following equation for ground roll distance to takeoff is obtained:

$$S_d = \{W/[\rho gS\cdot(\mu C_{L_g} - C_{D_g})]\}\cdot \mathrm{Ln}\{1 + V_{to}^2\cdot[(\rho S/2W)\cdot(\mu C_{L_g} - C_{D_g})]/[(T/W)\cdot(\cos(\theta_j+\alpha) + \mu\sin(\theta_j+\alpha)) - \mu]\} \quad (2)$$

Equation (2) additionally assumes takeoff occurs rapidly after thrust vectoring. A good estimate for time between V_v to V_{to} obtained from flight test is approximately 1 sec for 20,000 to 30,000 lb rapid thrust vectoring jet aircraft. The difference in takeoff distance resulting from the instantaneous takeoff assumption can be surveyed in order to determine the validity of this assumption for a given case.

Aircraft acceleration will decrease upon thrust vectoring mostly due to the reduction in thrust acting in the axial direction. Acceleration may also decrease if high lift devices (such as flaps) are scheduled to react with the vectored thrust (due to the increase in induced drag). In cases where vectored thrust is used in conjunction with high lift devices (such as flaps), the influences of thrust on C_{D_g} and C_{L_g} must also be accounted for. Aircraft acceleration changes between initiation of thrust vectoring and takeoff can be estimated from

$$\Phi = (V_{to} - V_v)/\Delta t = V\cdot dV/dS \quad (3)$$

Using $\Delta t = 1$ sec, and assuming ground roll acceleration (Λ) is constant, equation (3) can be rearranged and integrated to obtain

$$S_c = [(V_{to}^2 - V_v^2)/[2(V_{to} - V_v)] \quad (4)$$

The error associated with the instantaneous takeoff assumption ($S_v = S_g$) can be estimated using

$$S_e(\%) = [S_c/(S_d + S_c)]\cdot 100 \quad (5)$$

Constant ground roll acceleration can be determined from

$$\Lambda = [T\cos(\theta_j+\alpha) - D_g - \mu(W - L_g - T\sin(\theta_j+\alpha))]\cdot(g/W) \quad (6)$$

The assumption of constant ground roll acceleration does not necessarily over simplify the ground roll distance equation. Variation of forces acting on the aircraft during ground run are shown in figure 3. With low takeoff velocities associated STO operations, assume net thrust will remain reasonably constant over the ground run (minimum change in T due to a change in momentum drag over the ground run). As lift develops, drag increases and $\mu(W - L - T\sin(\theta_j+\alpha))$ decreases. Even though these forces cannot be shown to directly cancel, the net difference in these forces will remain reasonably constant during the takeoff, particularly for short takeoff distances. As in the constant thrust assumption, Λ should be calculated at conditions where the velocity is equal to $V_{to}/\sqrt{2}$.

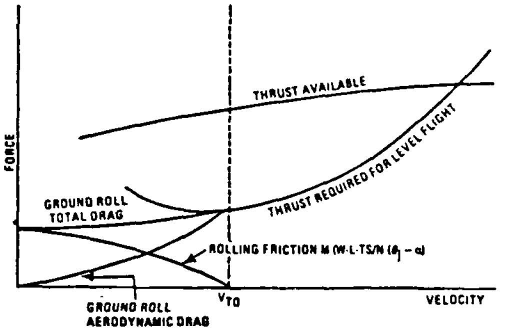

Figure 3 Variation Of Forces During Ground Roll

Flight test takeoff data obtained from Harrier STO testing supports the validity of the constant ground roll acceleration assumption. Assuming the ideal case where gross thrust is the only force acting on the aircraft during the ground run in the direction of the velocity vector, the work-energy expression becomes

$$1/2\cdot(W/g)\cdot V^2 = T_g\cdot S_d = (W/g)\cdot a\cdot S_d$$

By rearranging the terms, the expression becomes

$$a = 1/2\cdot(V^2/S_d)$$

Therefore, the acceleration is linearly proportional to V^2/S_d. Multiplying both sides of the equation by W/g and rearranging the terms gives

$$2gS_d = (W/T_g)\cdot V^2$$

The term $(W/T_g)\cdot V^2$ is commonly referred to as the acceleration parameter. W/T_g can be replaced by hover weight ratio, W/W_h. Hover weight, W_h, is defined as the maximum weight at which the aircraft can remain in a steady hover condition for the given ambient conditions. An advantage of W/W_h is that it can be accurately obtained through relatively simple flight testing. Disregarding the effects of the pressure differential between the top and bottom of the aircraft during a hover (resulting from thrust vectored under the aircraft), installed maximum available gross thrust less any engine bleed required during hover conditions is equal to W_h. Assuming bleed effects are minimal, W/T_g is replaced by W/W_h.

With this substitution, the above expression shows that $(W/W_h)\cdot V^2$ is linearly proportional to S_d. By further rearranging the terms, the expression can be written as

$$(W/W_h)\cdot(V^2/S_d) = 2g$$

Therefore, assuming a constant hover weight ratio over the ground run for the ideal case, aircraft acceleration is constant.

Plotting $(W/W_h)\cdot V^2$ versus S_d from actual STO data has shown that $(W/W_h)\cdot V^2$ is linearly proportional to S_d (representative curve shown in figure 4). Note however that since maximum thrust available is finite, as vehicle gross weight increases to the point where hover weight ratio increases significantly, the curve becomes less linear. This effect is due mostly to the significant increase in aerodynamic drag resulting from the higher takeoff velocities required for the lift necessary to offset the higher gross weights. The effect also occurs as a result of increased momentum drag. At the point of degrading linearity, the constant ground roll acceleration assumption becomes less valid.

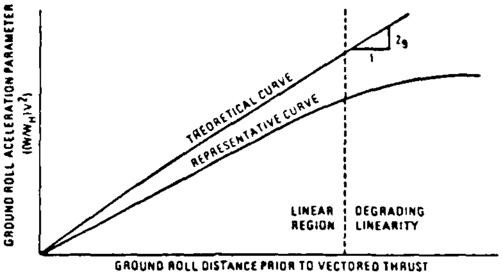

Figure 4 Ground Roll Acceleration Curve

Using the constant Λ assumption, equation (1) can be integrated and rearranged to become

$$S_d = V_{to}^2/(2\Lambda) \tag{7}$$

Again, this assumes takeoff occurs quickly after thrust vectoring. However, equation (4) can be used to estimate S_c. The advantage of equation (7) is that S_d can be analyzed relative to Λ, thus determining the effects of different accelerations on ground roll distance. As will be shown, this becomes more useful for the air distance equation.

Variation Of Lift And Drag With Ground Roll Distance

For analysis purposes, L and D can be expressed as a function of S_d. The rate of change of drag with ground roll distance can be expressed as

$$dD/dS_d = (dD/dV\cdot dV/dt)/(dS_d/dt)$$

Substituting in,

$$dD/dV = d/dV(1/2\rho V^2SC_{D_g}) = \rho VSC_{D_g}$$
$$dV/dt = [T\cos(\theta_j+\alpha) - D_g - \mu(W - L - T\sin(\theta_j+\alpha))]\cdot(g/W)$$
$$dS_d/dt = V,$$

simplifies to

$$dD/dS_d = \rho SC_{D_g}[T\cos(\theta_j+\alpha) - D_g - \mu(W - L - T\sin(\theta_j+\alpha))]\cdot(g/W)$$

Relationships of the variables in dV/dt to S_d can be substituted in for best results. A more simplified version can be obtained by assuming C_L, C_D, and W remain constant over the ground run, and using the constant Λ assumption. Integrating with respect to ground roll distance gives the following:

$$D(S_d) = \rho SC_{D_g}\Lambda S_d \tag{8}$$

Knowing $L = 1/2\rho V^2SC_L$, a similar approach yields

$$L(S_d) = \rho SC_{L_g}\Lambda S_d \tag{9}$$

Determination Of Velocity For Thrust Vectoring

In theory takeoff occurs when the total lift is equal to the aircraft weight ($W = L_t$). Therefore V_{to} would be the velocity corresponding to the point where

$$L_t = 1/2\rho V_{to}^2SC_{L_g} + T_g\sin(\theta_j+\alpha) \tag{10}$$

for some given T_g resulting from a takeoff power throttle setting. Because thrust vector angles used for takeoff will be large, the net thrust term is broken into the gross thrust and momentum drag terms due to the respective differences relative to the flight path. For drag bookkeeping purposes, momentum drag is commonly resolved in the direction of the velocity vector (perpendicular to L_t).

Takeoff velocity for determining the ratio of wing lift to thrust lift is very important. If minimum wingborne lift is used, a larger θ_j is required, thus allowing less thrust for acceleration during transition from semijetborne flight (flight requiring both aerodynamic and thrust generated lift) to wingborne flight (flight requiring aerodynamic lift only) during climbout. Also, if takeoff velocity is such that maximum lift available from the wing is required for $W = L_t$, angle of attack will be large creating additional induced drag and a potential stall hazard. Therefore, the balance of wing lift and thrust lift is critical not only for takeoff, but for climbout characteristics as well.

The key to STOL operations is not necessarily to takeoff in the minimum distance required, but to takeoff and climb out above some height in the least possible distance while maintaining adequate flight path acceleration for continuing the climb to desired altitude. If the wing lift to thrust lift ratio is not optimum for the STO technique, the pilot may takeoff in the minimum distance required, but he may significantly increase that distance trying to accelerate and climb above an obstacle. The STO technique also has a direct impact in optimizing the STO task for minimum distance required to clear a given height while maintaining a reasonable flight path acceleration.

Another variable impacting STO performance is engine operating limitations (temperature, RPM, etc.). Takeoff velocity should allow flight path acceleration to minimize the time required to adequately perform the STO task such that engine life is not reduced and/or thrust reduction does not occur due to reaching or exceeding engine operating limits during climbout and transition to wingborne flight.

The velocity at which a pilot vectors thrust in order to initiate takeoff is V_v. Assumptions can be made to simplify equation (10) allowing the development of a thrust vector velocity schedule relating takeoff velocity with thrust available, thrust vector angle, and gross weight for some predetermined STO technique. Substituting in $L_t \geq W$ at takeoff, replacing W/T_g with W/W_h, and rearranging the terms gives

$$(V_v/\sqrt{W}) \geq \sqrt{[2\cdot(1 - [1/(W/W_h)]\cdot\sin(\theta_j+\alpha))/(\rho S C_{L_g})]} \qquad (11)$$

The term $V_v/\sqrt{W}$ is termed the velocity parameter. Equation (11) shows that velocity parameter is a function of only hover weight ratio for a given STO technique where thrust is vectored to the same θ_j and α at takeoff is consistent for all gross weights (i.e., target θ_j and α are a result of the STO technique). From this, a schedule depicting velocity for thrust vectoring can be estimated and presented as $V_v/\sqrt{W}$ versus W/W_h as shown in figure 5. If takeoff was assumed to occur at the instant that thrust was vectored, V_v could be replaced with V_{to}. However, recall that the determination of the takeoff velocity (a direct relation with V_v) is a function of the STO technique as well as the lift and thrust performance of the aircraft. While addressing constraints due to the STO technique, equation (11) can be used to estimate a takeoff schedule prior to actual STO testing.

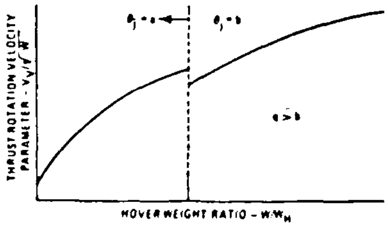

Figure 5 Thrust Vector Rotation Velocity Schedule

If the STO technique is an attitude takeoff task (i.e., thrust is vectored at V_v and takeoff occurs shortly afterwards without rotation of the nose (as is usually required with conventional takeoff aircraft), then ground run pitch attitude can be substituted into equation (11) for α.

Prediction Of Ground Distance Required To Clear An Object During Takeoff Air Phase

In order to determine the total distance required to clear an obstacle during a STO, the air phase distance must be accounted for separately from the ground roll phase distance due to the difference in the forces acting on the aircraft.

The free body diagram for an aircraft in flight is shown in figure 6. Applying the work-energy relationship gives the following expression

$$\int[T_g\cos(\theta_j+\alpha) - D - D_M]\cdot dS_d - (W_2h_2 - W_1h_1) = \int(W/g)\cdot V dV \qquad (12)$$

The subscript 1 defines the datum at the takeoff position as 0 ft above ground level (AGL), and subscript 2 is at 50 ft AGL level. If the weight change between takeoff and 50 ft AGL is assumed negligible, then gross weight is a constant.

Applying this assumption, equation (12) can be simplified to

$$\int[T_g\cos(\theta_j+\alpha) - D - D_M]\cdot dS_d = [W/(2g)]\cdot[V_{50}^2 - V_{to}^2 - 100g] \qquad (13)$$

Ideally, for the determination of flight path distance (S_{fp}) required to clear 50 ft AGL, relationships of D, D_M, θ_j, and α to S_d between takeoff and 50 ft AGL would be required for solving equation (13). These variables are directly related to flight path acceleration, and are therefore critical relative to STO performance optimization.

As shown for the ground roll case, certain assumptions can be applied to equation (13) in order to develop a more simplified form. Because the optimization of STO performance will result in low, but acceptable flight path acceleration, and as a result of the position capture climbout task during the air phase portion of the STO, assume α, C_D, and D_M remain fairly constant over the climbout to 50 ft AGL. Also, assume that Tg will not vary during climbout. Furthermore, assume that the thrust vector angle is constant throughout the climbout. If acceleration is adequate, the pilot may begin to vector the thrust aft and transition to wingborne flight prior to 50 ft AGL. Relative to available flight path acceleration for the given climbout angle, the constant θ_j assumption during climbout is the worse case situation. However, if the pilot transitions to wingborne flight too soon, the aircraft could begin to descend due to the deviation from optimum L_t conditions.

Since all the variables within the integral are assumed to be fairly constant throughout the climb, the non-conservative forces are now presented as

$$F_{avg} = [T_g\cos(\theta_j+\alpha) - D - D_M]_{avg}$$

As in the ground roll equation, the parameters assumed to be constant over the air phase should be evaluated at average conditions occurring at $\sqrt{([V_{50}^2 + V_{to}^2]/2)}$. Integrating and rearranging equation (13) gives the following expression

$$S_{fp} = [W/(2gF_{avg})]\cdot[V_{50}^2 - V_{to}^2 - 100g] \quad (14)$$

Therefore, the ground distance covered during climbout is

$$S_{ap} = S_{fp}\cdot\cos\gamma_g \quad (15)$$

For no wind conditions, the angle γ_g can be calculated from

$$\arcsin(V_y/V_t) = \gamma_g \quad (16)$$

Applying equation (15) to equation (14), the following is obtained:

$$S_{ap} = [W/(2gF_{avg})]\cdot[V_{50}^2 - V_{to}^2 - 100g]\cdot\cos\gamma_g \quad (17)$$

The simplified version of the air phase distance equation is useful for minimizing S_{ap} relative to the variables contained in F_{avg}. In other words, the variables governing F_{avg} can be manipulated within the given constraints of the aircraft in order to minimize the distance required for climbout.

Environmental Effects on STO Performance Prediction

Ambient conditions can greatly affect takeoff performance. Because the equations predicting takeoff distance and distance required to clear 50 ft AGL are derived from the work energy relationship, they assume that airspeed is equal to inertial ground velocity (no wind conditions). The equations also have not accounted for any runway slope. In addition, the distance calculated is for some given density condition which affects thrust, lift and drag. Takeoff performance can be adjusted to any ambient conditions using empirical methods. The corrections are not within the scope of this paper; however, reference 2 discusses how to correct takeoff performance to desired conditions relative to environmental effects.

Relationship Of The Flight Path Acceleration Parameter To STO Performance

The most important aspect of the STO task is maintaining acceptable flight path acceleration during climbout. It will be shown that when performing a STO at a W/W_h below the W/W_h for design optimum STO task conditions, a/g will be above acceptable conditions. At some W/W_h above the W/W_h for design optimum STO task conditions, a/g will fall below acceptable conditions. The W/W_h for which a/g becomes unacceptable can be determined by comparing the velocity required for the climbout task with the velocity required for minimum acceptable a/g (dictated by the given STO technique). The following paragraphs outline the flight test technique utilized in predicting the W/Wh for which a/g becomes unacceptable for the design optimum STO technique.

Flight path acceleration can be determined from constant airspeed climb tests. A free body diagram of an aircraft in flight is shown in figure 6. Summing the forces along the flight path for a constant airspeed climb gives

$$\Sigma F_x = T_g\cos(\theta_j+\alpha) - D - D_M - W_C\sin\gamma = (W_C/g)\cdot a_x = 0 \quad (18)$$
$$\Sigma F_y = T_g\sin(\theta_j+\alpha) + L - W_C\cos\gamma = (W_C/g)\cdot a_y = 0 \quad (19)$$

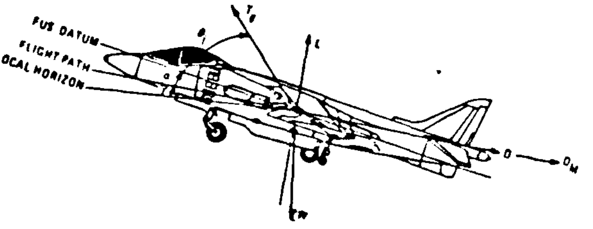

Figure 6 Forces On Aircraft During Flight

Therefore,

$$D/L = [T_g\cos(\theta_j+\alpha) - W_C\sin\gamma - D_M]/[W_C\cos\gamma - T_g\sin(\theta_j+\alpha)]$$

Rearranging and solving for tan γ gives

$$\tan\gamma = \{[T_g\cos(\theta_j+\alpha) + (D/L)\cdot T_g\sin(\theta_j+\alpha) - D_M]/[W_C\cos\gamma] - (D/L)\} \quad (20)$$

Note that D/L can be replaced by C_D/C_L.

Summing the forces along the flight path for a level acceleration ($\gamma = 0$) gives

$$\Sigma F_x = T_g\cos(\theta_j+\alpha) - D - D_M = (W_L/g)\cdot a_x \quad (21)$$
$$\Sigma F_y = T_g\sin(\theta_j+\alpha) + L - W_L = (W_L/g)\cdot a_y = 0 \quad (22)$$

Therefore,

$$D/L = [T_g\cos(\theta_j+\alpha) - W_L\cdot(a_x/g) - D_M]/[W_L\cos\gamma - T_g\sin(\theta_j+\alpha)]$$

Rearranging and solving for a_x/g gives

$$a_x/g = \{[T_g\cos(\theta_j+\alpha) + (D/L)\cdot T_g\sin(\theta_j+\alpha) - D_M]/W_L - (D/L)\} = a/g \quad (23)$$

Because the lift and drag are different for climb and level flight, the relationship between the climb velocity and level flight velocity needs to be established in order to determine the velocity associated with the level flight a/g. From equations (19) and (22) lift can be expressed as

$$L_C = W_C\cos\gamma - T_g\sin(\theta_j+\alpha) = (1/2\rho V^2 SC_L)_C$$
$$L_L = W_L - T_g\sin(\theta_j+\alpha) = (1/2\rho V^2 SC_L)_L$$

So for $W_L = W_C\cos\gamma$, and assuming ρ, T_g, θ_j and S to be the same for both the climb and level flight situation, then

$L_C = L_L$. Therefore,
$C_{LC} = C_{LL}$. Therefore,
$\alpha_C = \alpha_L$. Therefore,
$V_C = V_L$. Therefore,
$D_C = D_L$. Therefore,
$(D/L)_C = (D/L)_L$. Therefore,
$D_{MC} = D_{ML}$.

Thus, the only difference between equations (20) and (23) right of the equal sign is the aircraft gross weight term in the divisor. The flight path angle obtained during constant airspeed climb tests can be related to level flight acceleration if $W_L = W_C\cos\gamma$. The relation can be written by

$$\tan\gamma = a/g \quad (24)$$

where $W_L = W_C\cos\gamma$, and the flight path angle γ during the climb test is determined from

$$\arcsin(V_y/V_t) = \arcsin\{(\Delta h/\Delta t)/V_t\} = \gamma \quad (25)$$

Equation (24) states that the flight path acceleration of an aircraft in level flight at weight W_L and velocity V_L can be determined from constant airspeed climb data for which $V_C = V_L$ and weight W_C is such that $W_L = W_C\cos\gamma$. Also, equations (23) and (24) can be used for the development and prediction of the thrust rotation velocity schedule. Note, since drag in level flight is higher than drag in climbing flight for similar aircraft at the same weight and velocity, the a/g calculated is a conservative estimate of a/g during climbout at the corresponding velocity.

The calculated level acceleration data can be adjusted for different gross weights. Acceleration correction, Δa/g, due to weight correction, ΔW, can be written as

$$\Delta W = W_D - W_L$$
$$\Delta(a/g) = (a/g)_D - (a/g)_L$$

Therefore,

$$\Delta(a/g) = \{[T_g \cos(\theta_j+\alpha) + (D/L)\cdot T_g \sin(\theta_j+\alpha) - D_M]/W - (D/L)\}_L - \{[T_g \cos(\theta_j+\alpha) + (D/L)\cdot T_g \sin(\theta_j+\alpha) - D_M]/W - (D/L)\}_D \quad (26)$$

Constant airspeed climbs at different weights have different angles of attack and momentum drag at the same thrust setting. If weight corrections are small (±5%), then it is not unreasonable to assume that the angles of attack for the given and desired weight conditions are equal. Therefore, V_D is assumed approximately equal to V_L; consequently, $(D/L)_D$ is approximately equal to $(D/L)_L$ and $(D_M)_D$ is approximately equal to $(D_M)_L$. Although the desired weight condition has the same angle of attack, thrust setting, and approximately the same velocity as the original condition, an algebraic difference in a/g results because the relative pitch attitude changes due to the difference in weight (i.e., *because pitch attitude is equal to the* sum of α and γ, the different pitch attitude produces a change in γ, which in turn changes a/g). Applying the above assumptions to equation (26),

$$\Delta a/g \approx T_g \cdot [(W_D - W_L)/(W_D W_L)] \cdot \{\cos(\theta_j+\alpha) + (D/L)\cdot \sin(\theta_j+\alpha)\} \quad (27)$$

Recall again that D/L can be written as C_D/C_L. Note also that some cases may constitute a further simplification of equation (27) to

$$\Delta a/g \approx T_g \cdot [(W_D - W_L)/(W_D W_L)]$$

The difference between V_D and V_L (resulting from the weight change and constant angle of attack assumption) can be calculated. Solving equation (19) for T_g, substituting into equation (18), rearranging the expression and applying the assumptions used in developing equation (24) shows

$$V_L^2 = \{W_L \cdot [1 - \tan\gamma \cdot \tan(\theta_j+\alpha)] - D_M \cdot \tan(\theta_j+\alpha)\}/[(C_D \cdot \tan(\theta_j+\alpha) + C_L)\cdot(1/2)\rho S] = V_C^2 \quad (28)$$

Doing the same for the desired weight condition yields

$$V_D^2 = \{W_D \cdot [1 - \tan\gamma \cdot \tan(\theta_j+\alpha)] - D_M \cdot \tan(\theta_j+\alpha)\}/[(C_D \cdot \tan(\theta_j+\alpha) + C_L)\cdot(1/2)\rho S] \quad (29)$$

Dividing equation (28) by equation (29) and applying equation (24) produces

$$(V_L/V_D)^2 = (W_L/W_D)\cdot\{[1 - (a/g)_L \cdot \tan(\theta_j+\alpha)] - D_M \cdot \tan(\theta_j+\alpha)\}/\{[1 - ((a/g)_L + \Delta(a/g))\cdot \tan(\theta_j+\alpha) - D_M \cdot \tan(\theta_j+\alpha)]\} \quad (30)$$

Applying the previous assumptions valid for a small weight correction allows

$$1 \approx \{1 - (a/g)_L \cdot \tan(\theta_j+\alpha) - D_M \cdot \tan(\theta_j+\alpha)\}/\{1 - ((a/g)_L + \Delta(a/g))\cdot \tan(\theta_j+\alpha) - D_M \cdot \tan(\theta_j+\alpha)\}$$

Therefore,

$$V_D = V_L \cdot \sqrt{(W_D/W_L)} = V_C \cdot \sqrt{\{W_D/(W_C \cdot \cos\gamma)} \quad (31)$$

The variables used to express a/g can be collected as independent, non-dimensional parameters in order to better evaluate aircraft performance. From equation (23)

$$a = f(T_g, \theta_j, \alpha, g, D/L, D_M, W) \quad (32)$$

For a given aircraft, it can be shown from aerodynamic theory that,

$$D/L = f(\alpha, \text{Mach Number}, \text{Reynolds Number})$$

Since this problem is restricted to low speed flight, an incompressible fluid at some constant ambient density is assumed. Therefore D/L can be expressed as

$$D/L = f(\alpha, V, x)$$

and

$$\alpha = f(W, V)$$

Substituting into equation (32) and assuming θ_j is constant lets

$$a = f(T_g, V, g, D_M, W, x)$$

Since W = mg and $D_M = MV$, level flight path acceleration data from constant airspeed climbs can be expressed as

$$a = f(T_g, V, g, M, m, x) \quad (33)$$

Equation (33) can be defined as

$$f(a, T_g, V, g, M, m, x) = 0 = f(\pi_1, \pi_2, \pi_3, \pi_4)$$

where
$$\pi_1 = f(T_g, V, g, a) = T_g^a \cdot V^b \cdot g^c \cdot a^1$$
$$\pi_2 = f(T_g, V, g, m) = T_g^a \cdot V^b \cdot g^c \cdot m^1$$
$$\pi_3 = f(T_g, V, g, x) = T_g^a \cdot V^b \cdot g^c \cdot x^1$$
$$\pi_4 = f(T_g, V, g, M) = T_g^a \cdot V^b \cdot g^c \cdot M^1$$

For $\pi_1 = T_g^a \cdot V^b \cdot g^c \cdot a^1$, the non-dimensional expression can be written as

$$\pi_1 = [MLt^{-2}]^a \cdot [Lt^{-1}]^b \cdot [Lt^{-2}]^c \cdot [Lt^{-2}]^1 = M^0 L^0 t^0 \quad (34)$$

Therefore,

M^0 $0 = a$
L^0 $0 = a + b + c + 1$
t^0 $0 = -2a - b - 2c - 2$

Solving for a, b, and c, and inserting the values back into equation (34) gives

$$\pi_1 = a/g$$

Doing the same for the other three non-dimensional variables yields

$$\pi_1 = a/g$$
$$\pi_2 = mg/T_g = W_L/T_g$$
$$\pi_3 = gx/V_L^2$$
$$\pi_4 = V_L M/T_g = D_M/T_g$$

So,

$$f(\pi_1, \pi_2, \pi_3, \pi_4) = 0 = f(a/g, W_L/T_g, gx/V_L^2, D_M/T_g)$$

Therefore,

$$a/g = f(W_L/T_g, gx/V_L^2, D_M/T_g) \quad (35)$$

If the aircraft is further constrained to a constant configuration, then the following expression can be written due to the fact that c.g. position is directly related to gross weight.

$$x = f(W) = f(m, g)$$

For this case, W varies only with the fuel state of the vehicle. The non-dimensional parameter, π_3, can be rearranged using x = f(W) by substituting in m for x, noting that g is already accounted for, such that the dimensional velocity parameter (previously defined) is obtained as

$$\pi_3' = V_L/\sqrt{W_L}$$

Therefore, a/g can be expressed as

$$a/g = f(W_L/T_g, V_L/\sqrt{W_L}, D_M/T_g) \tag{36}$$

Assuming changes in D_M/T_g to be negligible over the range of velocities involved, the expression can be further reduced to

$$a/g = f(W_L/T_g, V_L/\sqrt{W_L}) \tag{37}$$

Therefore, a/g is primarily a function of thrust to weight ratio and velocity parameter. For a given minimum acceptable a/g and recalling the concept of the hover weight ratio, equation (37) can be written as

$$(V_{a/g}/\sqrt{W}) = f(W/T_g) = f(W/W_h) \tag{38}$$

Setting the Kollsman window of the test altimeter to 29.92 in Hg prior to constant airspeed climb tests allows obtaining the standard day graph of $V_{a/g}/\sqrt{W}$ versus a/g from test day data of $V_{a/g}/\sqrt{W}$ versus a/g plotted in terms of test day equivalent airspeed. Variations in a/g due to differences in engine thrust resulting from ambient temperature and pressure effects are accounted for due to plotting a/g data relative to W/W_h. As usual, for best results tests should be performed as close to desired conditions (temperature, pressure, weight, etc.) as possible.

Relationship Of Climbout Task With STO Performance

Earlier, equation (11) showed that takeoff velocity was related to the STO task by

$$(V_{\surd}/\sqrt{W}) \geq \sqrt{}[2\cdot(1 - [1/(W/W_h)]\cdot\sin(\theta_j+\alpha))/(\rho S C_{L_g})] \tag{11}$$

For a given optimum STO technique, equation (11) becomes

$$(V_{\surd}/\sqrt{W}) = f(W/W_h) \tag{39}$$

Using equation (19), lift during the climbout phase of the STO is expressed as

$$L = (W/g)\cdot a_y + W\cos\gamma - T_g \sin(\theta_j+\alpha) = (1/2)\rho V^2 S C_L$$

By rearranging the terms and substituting in W/W_h, the velocity during the climbout task can be expressed as

$$(V/\sqrt{W}) \geq \sqrt{}[2\cdot((a_y/g + \cos\gamma) - [1/(W/W_h)]\cdot\sin(\theta_j+\alpha))/(\rho S C_L)] \tag{40}$$

The STO task profile defined climbout at a constant attitude or AOA, and in the case of constant attitude climbout, α is assumed to remain fairly constant. As assumed in the development of equation (14), θ_j is constant during climbout. Because the climbout phase of the STO task is relative to clearing an obstacle of reasonably low height (less than 100 ft), density also is assumed to remain constant over the climbout. Also, since STO performance is to be optimized within minimum acceptable a/g, assume $(a_y/g + \cos\gamma) = 1$. Therefore, velocity required for the climbout task can be expressed as

$$(V/\sqrt{W}) = f(W/W_h) \tag{41}$$

Optimum STO Performance

Prediction

As discussed earlier, optimum STO performance is governed by *minimum acceptable a/g available during the STO task.* Equations (39) and (41) formulate the approach to optimizing STO performance, and determining W/W_h for which a/g becomes unacceptable.

To maximize STO performance, an engineer can manipulate and fix the key variables in equations (4), (7), (11), (17), (23) and (40) as necessary in order to aid in the development of the initial thrust vector velocity schedule for optimum STO performance. Equations (2) and (13) could then be used to predict the associated distance performance. Again, recall that STO performance is directly influenced by handling qualities as well. Therefore, the variables in the above mentioned equations would also be constrained by the requirements of the STO task (i.e., adequate acceleration for climbout, task repeatability, reduced complexity, and minimum pilot workload). The average pilot must be able to execute the STO task with consistent results without the complexity of the task being overwhelming. When the variable combinations of the derived takeoff equations are set such that maximum STO performance is achieved relative to the chosen STO technique, predicted STO performance is considered optimized.

However, the variable combinations for optimum performance will change with W/W_h. In order to reduce the complexity involved in optimizing performance for every possible condition, the STO task is designed along with the constraining variables for operational conditions most likely encountered during the mission of the vehicle. For off-design conditions, the task remains constant (reducing operational complexity) until performance degrades below acceptable conditions. At this condition, selected parameters pertaining directly to vehicle performance can be varied in order to maintain the best possible STO performance for the determined STO task. Because the vehicle is performance constrained by the engine and aerodynamically constrained by geometry, off-design performance can be optimized by changing the target engine thrust vector angle. In order to optimize aircraft handling qualities, longitudinal trim setting for takeoff is varied to obtain the best aircraft response for quick takeoff upon thrust vectoring, and precise attitude targeting and control during climbout.

Determination

Unlike conventional takeoff testing, it is difficult to separate *STO testing of vectored thrust aircraft into distinct flying* qualities and performance tests. The repeatable STO task is directly dependent upon both aircraft performance and STO technique (which includes climbout as well as takeoff). In order to achieve repeatability of optimum STO performance, the STO task must optimize aircraft performance relative to lift, drag, thrust and acceleration, and at the same time balance in the requirements of quick and precise attitude capture, attitude control and maximum available rate of climb.

Constant airspeed climb tests are performed at a given thrust vector angle to obtain plots of velocity parameter versus a/g for various lines of constant hover weight ratio (figure 7). The velocity parameter at which the predetermined minimum acceptable a/g occurs is then cross plotted against W/W_h (figure 8). This plot is then overlaid onto a plot of velocity parameter required during climbout at the captured attitude or AOA versus W/W_h, obtained for the same target thrust vector angle as used during the constant airspeed climb tests (figure 9). If the curves depicting velocity parameter required for the climbout task and the velocity parameter for minimum acceptable a/g intersect at a W/W_h within the operational hover weight ratio envelope,

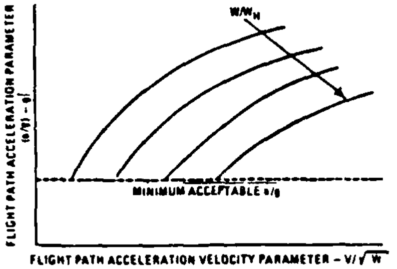

Figure 7 Determination Of Velocity For Minimum Acceptable a/g For A Given Target Thrust Vector Angle

acceleration is no longer acceptable for the given optimum STO technique utilizing that target thrust vector rotation angle. The hover weight ratio at which the velocity parameter for minimum acceptable a/g equals the velocity parameter required for the climbout task is defined as the thrust vector angle crossover point. If desired, a safety buffer can be utilized in the determination of the thrust vector angle crossover point as shown in figure 9.

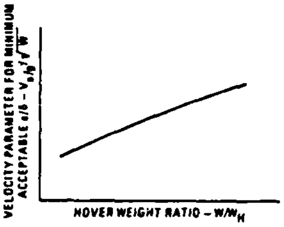

Figure 8 Velocity For Minimum Acceptable a/g Versus W/W_h For A Given Thrust Vector Angle.

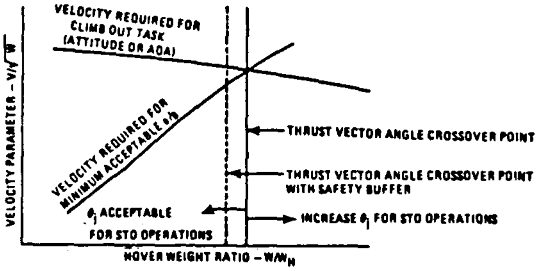

Figure 9 Determination Of Thrust Vector Angle Crossover Point

At this point, the variables in the takeoff equations could be reexamined in order to develop a new STO technique for hover weight ratios in excess of thrust vector angle crossover point. For a given vehicle, there is a finite maximum available thrust and maximum allowable gross weight for takeoff. Therefore, the two major ways of improving a/g are to vary vector thrust angle and angle of attack. Angle of attack during ground run is a function of vehicle attitude as long as the vehicle rests on the landing gear. For climbout, the angle of attack will depend on the STO technique. As stated earlier, the situation may dictate that the design STO technique will remain consistent for all hover weight ratios in order to reduce complexity of aircraft operation. Therefore, at the thrust vector angle crossover point the target thrust vector rotation angle would be reduced allowing for higher axial acceleration.

Constant airspeed climb tests are then performed for the new thrust vector angle in order to produce the required plots as previously discussed for the initial θ_j. If the new curves depicting velocity parameter required for the climbout task (relative to the new θ_j) and the velocity parameter for minimum acceptable a/g intersect at a W/W_h still within the operational hover weight ratio envelope, acceleration is no longer acceptable for the given optimum STO technique utilizing this new θ_j. Therefore, another reduction in target nozzle rotation angle is required for W/W_h above the second thrust vector angle crossover point. The process would then be repeated in order to determine if another reduction in θ_j is required to keep acceleration adequate, until the requirements for minimum acceptable a/g were satisfied for all W/W_h within the operational hover weight ratio envelope. The target thrust vector angles and corresponding hover weight ratios depicting the thrust vector angle crossover points are the components of the target thrust vector angle schedule. This schedule is used in conjunction with the thrust vector rotation velocity schedule during STO operations.

The initial (theoretically predicted) schedule for thrust vector rotation velocity can be compared to the velocity required for minimum acceptable a/g (obtained from flight test). Predicted V_v should be scheduled to occur at or above the velocity for acceptable level flight path acceleration such that the vehicle has adequate energy for transition to wingborne flight during climbout (thus minimizing ground distance required). If the initial schedule satisfies this criteria, it could be used as the starting point for determination of the final schedule from flight test. Depending on the confidence in the development of the initial schedule,it may be desired to add a safety buffer of 5 to 10 knots to the initial schedule prior to flight testing. Since maximum STO performance is desired, the final schedule for thrust vector rotation velocity should be approximately the same as curve depicting the velocity required for minimum acceptable a/g.

Application Of Technique

Background

YAV-8B and AV-8B STO test results had indicated that the STO performance could be further optimized, particularly at higher hover weight ratios (1.3 and above). Fleet comments and earlier STO test results confirmed the need for land based AV-8B STO performance optimization. STO optimization required the development of a new nozzle rotation schedule and STO task.

Description Of Test Aircraft

This above technique was applied for the determination of optimum STO performance of the AV-8B Harrier II aircraft. The AV-8B is a single place, single engine, tactical attack, vectored thrust V/STOL aircraft. The aircraft has a shoulder mounted supercritical swept wing, a single row of auxiliary engine air inlets, four rotatable engine exhaust nozzles, and a Lift Improvement Device System. The AV-8B is powered by a Rolls Royce F402-RR-406 twin spool, axial flow turbofan engine with an uninstalled sea level static short lift wet (water injection) thrust rating of 21,500 lb. The primary flight control system is hydromechanical with a limited authority digital stability augmentation and attitude hold system incorporating a departure resistance system. The Harrier also incorporates a reaction control system providing engine bleed air to puffer duct valves located on the nose, tail and wingtips for longitudinal, lateral and directional control during vectored thrust operations. The engine is equipped with a digital engine control system with a manual fuel system provided for back-up fuel control.

Test Approach

In order to achieve optimization, the STO task was changed to a pitch attitude capture task as opposed to the previous AOA task, and the target thrust vector angle (defined as nozzle rotation angle, θ_j) when used in reference to the AV-8B) was scheduled as a function of the hover weight ratio as opposed to being constant at 55 deg for all W/W_h. Constant airspeed climb tests were performed in order to determine the relationship between hover weight ratio and optimum nozzle angle during the STO task. This allowed the development of a new schedule for the velocity at which nozzles would be rotated (V_{nr}).

In order to maintain adequate flight path acceleration during high hover weight ratio STO tasks, the target nozzle angle was reduced, resulting in a slight increase in V_{nr}. The reduced nozzle angle increased flight path acceleration, while the increased V_{nr} provided more wing lift to supplement the reduced thrust lift (resulting from the reduction in nozzle angle).

The new optimum STO performance task outlined the STO task as rotating nozzles at V_{nr} (obtained from the developed V_{nr} schedule) to optimum target nozzle angle, capturing 14 deg pitch attitude within 1.5 sec of takeoff, and climbing through 50 AGL within minimum ground distance. Emphasis was placed on a repeatable STO task ending with sufficient acceleration at 50 ft AGL. Stabilator trim, drag and stability effects of stores, flight path acceleration, and flying qualities were all considered in the development of the revised nozzle rotation schedule. A new stabilator trim schedule was developed to enhance the pitch capture task in order to promote repeatability of the STO task. The schedule needed to account for drag and stability effects of stores, c.g. position, and potential reaction control system induced foreign object debris engine damage.

The STO task originally dictated application of the longitudinal stick as necessary to reach and maintain 12 units AOA after nozzle rotation and takeoff. However, previous test results showed that a reduction in flight path angle was required to maintain positive longitudinal flight path acceleration. Further testing was recommended in order to determine the optimum AOA for STO climbout. However, during the AV-8B Navy Technical Evaluation, it was determined that STO tasks capturing pitch attitude with proper trim were easier than capturing AOA due to the lag in the AOA indication in the HUD, and the tendency for the pilot to induce oscillations in AOA when targeting an AOA for climbout. Target pitch angle was chosen in order to optimize climbout AOA during higher hover weight ratio STO operations, as well as to maintain similarity with shipboard STO procedures.

Both the optimum and original STO tasks outlined STO procedures as initially setting proper control surface trim, selecting proper flap setting, selecting proper nozzle angle setting for the ground roll, applying appropriate power with brakes applied, releasing brakes at initial skid, accelerating to target V_{nr}, rotating nozzle lever to the pre-selected nozzle angle STO stop, and performing an attitude takeoff task. The main difference in task technique lies in capturing 14 deg pitch attitude within 1.5 sec for the optimum task as opposed to capturing 12 deg AOA for the original task. The tasks also have different V_{nr}, θ_j, and stabilator trim schedules. Both tasks call for maintaining altitude and heading during climbout.

Test Method

In order to determine the optimum nozzle rotation schedule, tests were conducted in two phases. The first phase involved the determination of the nozzle crossover point (the hover weight ratio for which the velocity parameter for minimum acceptable a/g equals the velocity parameter required for the 14 deg pitch attitude climbout task). The nozzle crossover point was determined by flying constant airspeed sawtoothed climbs at various hover weight ratios for 50 deg and 55 deg nozzle angles. Low pressure fan speed RPM was set during the climb in order to generate the required thrust for the targeted hover weight ratio. Constant airspeed climb data was then used to determine the velocity required to maintain a 14 deg pitch attitude and the velocity for minimum acceptable a/g. From experience gained during shipboard trials, the minimum acceptable a/g was chosen to be 0.04 g. During STO tests 0.04 g was again confirmed to be the minimum acceptable flight path acceleration for STO operations. The nozzle angle crossover point was determined from the intersection of the curves depicting velocity parameter required for 14 deg pitch attitude climb and velocity parameter for minimum acceptable a/g as a function of W/W_h for STO operations targeting 55 deg θ_j.

The second phase of the testing was to determine the nozzle rotation schedule for the newly defined STO task. The major test criteria was to determine V_{nr} such that the total distance required to clear 50 ft AGL was minimum and a/g remained acceptable during climbout providing a repeatable STO task for the average pilot. As a result of the data obtained from the constant airspeed climb tests, initial test nozzle rotation velocities were chosen from the original nozzle rotation schedule plus 10 KTS. Tests were conducted in a build-up approach by performing lower hover weight ratio tests first. If aircraft flight path acceleration and handling qualities were qualitatively and quantitatively acceptable throughout the STO task, V_{nr} was decreased in 2 - 5 KT increments and the test was repeated. V_{nr} was reduced until minimum acceptable a/g was achieved or pilot comments indicated that any further reduction in V_{nr} would have adverse effects on the flying qualities and repeatability. Trim was initially set using the original trim schedule. During STO testing, trim was varied for each loading tested in order to develop the optimum trim schedule. A removable mechanical throttle stop was used so that engine RPM cutback did not occur due to engine temperature limiters, thus guaranteeing that the hover weight ratio would remain reasonably constant throughout the STO.

Test Results

Test data showed the nozzle angle crossover point to be at 1.35 W/W_h (with approximately 10 KCAS performance safety margin) for 55 deg θ_j. If a pilot were to perform a 14 deg pitch attitude climbout with 55 deg θ_j above 1.35 W/W_h, he would sense that the aircraft was not accelerating, and in fact the aircraft would begin to stagnate, inhibiting the pilot from transitioning from semijetborne flight to wingborne flight. Constant airspeed climb tests for 50 deg θ_j showed acceptable a/g for all W/W_h above the nozzle angle crossover point of 1.35 W/W_h. When the aircraft acceleration data was plotted against the current original V_{nr} curve, the results showed that the original curve would cause a pilot to be below the minimum acceptable a/g for a target V_{nr} at hover weight ratios above 1.30 for STO operations using 55 deg nozzle angle. Therefore, during the originally defined STO task, a pilot would begin to experience stagnation (lack of acceleration). Both fleet and test pilot comments prior to this evaluation supported this finding.

The final V_{nr} schedule was then plotted in the form of velocity parameter versus hover weight ratio, for corresponding regions of target θ_j. A comparison between data for the original STO task and the developed STO task depicting total ground distance required to clear 50 AGL at the same test conditions showed the distances to be approximately the same (within ±200 ft, positive for W/W_h below the nozzle angle crossover point, and negative for W/W_h above the nozzle angle crossover point). Therefore, new nozzle rotation schedule and trim schedule produced no major change in required distances, increased flight path acceleration, and provided adequate handling qualities allowing the pilot to perform a safe and repeatable STO for all operational hover weight ratios tested.

The lower hover weight ratio data showed that the distance to clear 50 ft AGL using the maximum STO performance was slightly more then the original STO method. This is a result of using the pitch attitude capture technique as opposed to AOA capture. The lower hover weight ratio tests were conducted at lower gross weights. This provided for lower angles of attack, thus lower rates of climb. However, the ability of the aircraft to accelerate in the axial direction was enhanced. Performance can be further optimized if pitch attitude (as well as θ_j) is optimized relative to hover weight ratio such that rate of climb is maximized while keeping adequate flight path acceleration. Performance could also be further optimized by just increasing target θ_j, resulting in a decrease in a/g. However, as stated earlier this increases the complexity of the STO task. Since the pitch attitude was chosen for the most likely operational condition, and because performance for lower hover weight ratio conditions was adequate, the constant pitch attitude capture task was considered acceptable for all operational hover weight ratios tested.

Conclusion

Using the concepts of thrust vector rotation schedule and minimum acceptable a/g allowed the development of an optimum STO technique with associated V_{nr} schedule, nozzle angle schedule, and stabilator trim schedule optimizing STO performance and producing a safe, repeatable STO task for all operational hover weight ratios. Advantages to the developed test approach included:

1. Increased flight test efficiency. Minimum flight testing was needed to determine the required thrust vector angle crossover points, thrust vector angle schedule, thrust vector rotation velocity schedule, and the trim schedule optimizing attitude capture for various loadings.

2. Development of a STO task accounting for both the handling qualities and performance constraints of a given test vehicle, therefore optimizing the performance and repeatability of the STO technique.

3. The concept of the velocity parameter and hover weight ratio reduced complexity of data presentation and documentation.

Additional benefits can be gained by applying the concept of minimum acceptable a/g along with the developed takeoff performance and a/g equations in order to analyze and develop an optimum STO technique accompanied with associated performance schedules prior to flight testing. This can be particularly useful in the early design phase of an aircraft and further benefits can be gained when applied in conjunction with simulation.

Acknowledgements

The author wishes to acknowledge Mr. C. Lea and Mr. L. Thomas of the Naval Air Test Center for their contributions to this investigation.

References

1. Kollsman, David L., "Introduction to V/STOL Airplanes", first ed., 1981.

2. "USAF Test Pilot School Flight Test Handbook, Performance; Theory and Flight Test Techniques", FTC-TIH-79-1, dated 1 Aug 79.

3. "Carrier Suitability Manual", NAVAIR 51-35-50.

DISTRIBUTION:

NAVAIRSYSCOM (5301)	(2)
NAVAIRSYSCOM (5117F)	(2)
NAVAIRSYSCOM (5363)	(2)
PACMISTESTCEN (3103)	(2)
COMOPTEVFOR (521)	(2)
AIRTEVRON FIVE	(2)
NAVPRO St. Louis, MO	(2)
NAVAIRTESTCEN (SA)	(5)
NAVAIRTESTCEN (SY)	(1)
NAVAIRTESTCEN (FW)	(1)
NAVAIRTESTCEN (RW)	(1)
NAVAIRTESTCEN (TPS)	(1)
NAVAIRTESTCEN (CT01A)	(2)
DTIC	(2)

END
DATE
FILMED
5-88
DTIC